ROTATION CORRECTION IN INTERFERENCE FITS CALCULUS

Gruescu Corina [1], Bodea Renata [2]
[1]University "Politehnica" of Timisoara, [2] University of Oradea,
corina.gruescu@mec.upt.ro, prod.conf@rdslink.ro

Keywords: interference fit, interference correction, angular velocity influence, FEM analysis.

Abstract: The paper deals with the problem of stress and strain within the shaft and hub of interference fits in rotation. The thick walled sleeves theory provides analytical expressions for stress and strain in static regime. Due to rotation movement, supplemental stress and deformation occur so that the interferences gets smaller and the fit loosening. The paper compares the correction recommended in the literature with the results of a FEM analysis. The conclusion is that for each application a numerical analysis is required, as the results of empirical recommendations are only approximate.

1. INTRODUCTION

Calculus of interference fits is based on thick sleeved walls theory. The interference expression of s_{min} is [1 – 3]:

$$S_{nec} = p^*_{min} \cdot d \cdot \left[\frac{1}{E_1}\left(\frac{d^2 + d_1^2}{d^2 - d_1^2} - \nu_1 \right) + \frac{1}{E_2}\left(\frac{d_2^2 + d^2}{d_2^2 - d^2} + \nu_2 \right) \right] \cdot 10^3 \ \ [\mu m], \qquad (1.1)$$

where s_{nec} – necessary interference p^*_{min} – minimum contact pressure, d, d_1, d_2 – nominal diameters of the fit parts (fig. 1), $\nu_{1,2}$ – Poisson coefficient of materials, $E_{1,2}$ – elasticity modules of materials.

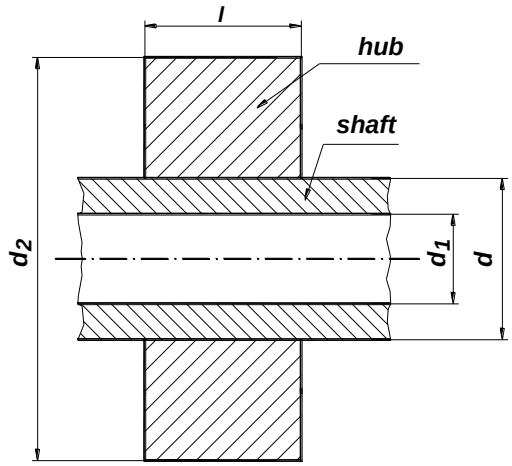

Figure 1 Shaft and hub of an interference fit and characteristic nominal diameters

The required interference results through adding at least three interference corrections to the minimum one [1-3]:

$$s_{min\ req} = s_{nec} + s_R + s_T + s_\omega \ldots, \qquad (1.2)$$

where s_R – correction due to roughness of the surfaces in contact, s_T – correction due to working temperature of the fit, s_ω - correction due to rotation.

Rotation may represent an important element to influence the interference fit. This aspect is considerably noticed for high rotation speeds or/and large sizes of the nominal fit.

The interference fit is affected by rotation because the later influences directly the contact pressure. Fundamentally, the rotation motion introduces a centrifugal force. It is an inertial force depending on the mass, angular velocity and distance to the rotation axis. The centrifugal force determines a pressure component, which algebraically sums with the static contact pressure. In hub's case, both pressure components are sign alike. Thus, its interior surface, supplementally stressed, is radially over deformed. In shaft's case, the rotation induced pressure takes inverse sign to the existing static contact pressure. The result is loosening of exterior shaft radial deformation.

There are very few analytical formulae to compute s_ω. One of them [4] gives the expression:

$$s_\omega = \frac{\gamma}{E}\frac{\omega^2}{16g} d\left(d_2^2 - d^2\right)(3+\nu), \tag{1.3}$$

where γ - specific weight of the materials, g – gravitational acceleration, ω - angular velocity of the assembly.

With any dynamic application, even if a numerical correction was not added, the limit rotation speed is compulsory to be verified. In [4], the limit angular velocity is expressed with the relationship:

$$\omega_{lim} = 4\sqrt{\frac{s_{min\ req}\cdot E}{d\frac{\gamma}{g}\left(d_2^2 - d_1^2\right)(3+\nu)}}, \tag{1.4}$$

where ω_{lim} – limit angular velocity to which the interference is compensated by the deformations due to centrifugal forces.

The stresses induced solely by rotation are [5]:

$$\sigma_r = \frac{3+\nu}{8}\frac{\gamma}{g}\omega^2\left(r_2^2 + r_1^2 + \frac{r_1^2 r_2^2}{r^2} - r^2\right), \tag{1.5}$$

$$\sigma_t = \frac{3+\nu}{8}\frac{\gamma}{g}\omega^2\left(r_2^2 + r_1^2 + \frac{r_1^2 r_2^2}{r^2} - \frac{1+3\nu}{3+\nu}r^2\right), \tag{1.6}$$

where σ_r – radial stress, σ_t – tangential stress, r=d/2, $r_1=d_1/2$, $r_2=d_2/2$ r - current radius.

Equations (1.5, 1.6) show a nonlinear variation in respect with the radius. The maximum radial stress occurs at $r = \sqrt{r_1 r_2}$:

$$\sigma_{r\,max} = \frac{3+\nu}{8}\frac{\gamma}{g}\omega^2(r_2 - r_1)^2, \tag{1.7}$$

$$\sigma_{t\,max} = \frac{3+\nu}{8}\frac{\gamma}{g}\omega^2\left(r_2^2 + \frac{1-\nu}{3+\nu}r_1^2\right). \tag{1.8}$$

For a solid shaft (d_1 = 0), maximum stresses are equal and occur in the center of the part:

$$\sigma_r = \sigma_t = \frac{3+\nu}{8}\frac{\gamma}{g}\omega^2 r_2^2. \tag{1.9}$$

2. FEM ANALYSIS OF STRESS AND STRAIN OF INTERFERENCE FITS IN ROTATION

Application of FEM analysis requires numerical data. The input data of the interference fit were:

- d = 28 mm
- d_1 = 8 mm
- d_2 = 60 mm
- l = 30 mm
- $E_1 = E_2 = 1.9995 \cdot 10^5$ MPa
- $\nu_1 = \nu_2 = 0.32$
- σ_r = 1482 MPa (limit strength)
- σ_c = 889 MPa (yield point)
- pressure induced by interference: 22 MPa
- ω = 750; 1500; 3500; 6000 rpm.

Radial and tangential stress and deformation at the outer surface of the shaft are presented in table 1.

Table 1. Stresses and deformation of the shaft

n [rpm]	σ_r (r)/ σ_r (r_1) [MPa]	σ_t (r)/ σ_t (r_1) [MPa]	$\sigma_{von\ Mises}$ (r)/ $\sigma_{von\ Mises}$ (r_1) [MPa]	u (r) [μm]
0	-21.85 -5.02	-25.81 -48.02	46.03 24.10	-1.32
750	-21.60 -4.10	-23.49 -41.18	38.50 21.53	-1.16
1500	-21.04 -1.82	-10.76 -19.1	18.43 11.25	-0.74
3500	-19.99 11.00	15.95 132.6	33.69 100.17	+2.50
6000	-8.80 47.00	110.31 444.31	134.10 392.46	+9.66

Figures 2 and 3 show the course of radial and tangential stress in respect with the radius for n=6000 rpm (blue), n=3500 rpm (red) and n= 750 rpm (green).

The numerical results and graphs confirm the theoretical approach. For instance, at 6000 rpm, the maximum radial stress is 128.4 MPa (applying 1.7) for r = 7.48 mm. The numerical analysis provides σ_r = 112.8 MPa, the result of algebraic addition of the stress due to rotation with the stress due to the contact pressure, which is σ_r = - 17.1 MPa for r = 7.48 mm.

The effects of rotation are obvious. The higher angular velocity gets, the higher stress increases, very far from linear dependence. The shrink at the surface of shaft gets smaller and beyond 1500 rpm turns into positive deformation.

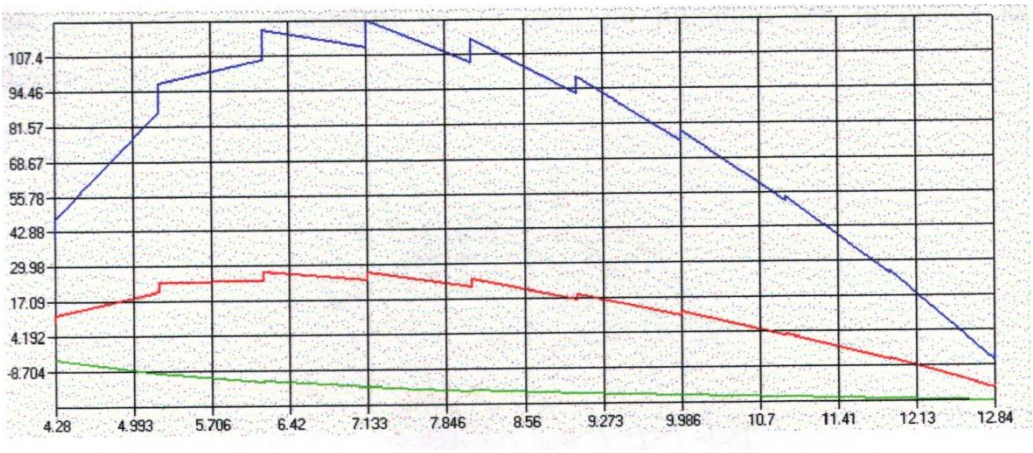

Figure 2 Shaft. Radial stress [MPa] at 750 rpm (green), 3500 rpm (blue) and 6000 rpm (red)

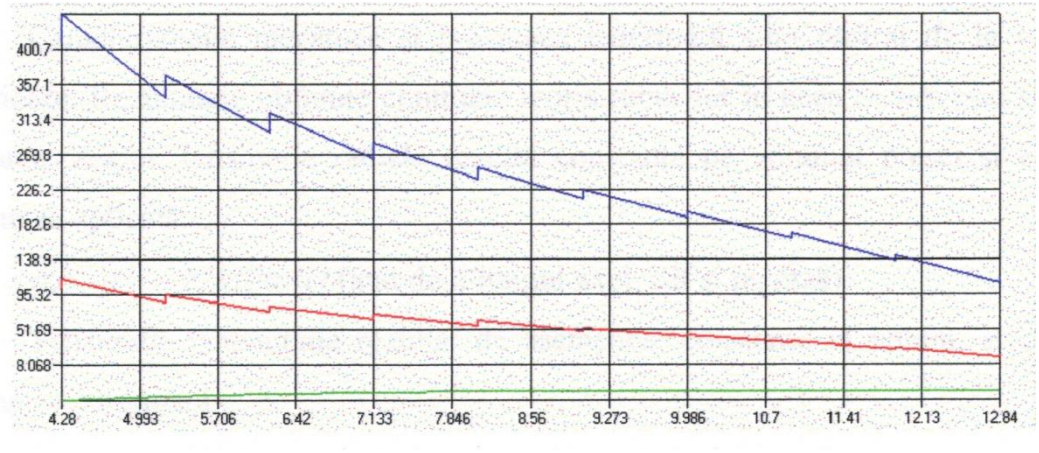

Figure 3 Shaft. Tangential stress [MPa] at 750 rpm (green), 3500 rpm (blue) and 6000 rpm (red)

Similar conclusions regarding the stresses result also for the hub. Figures 4 and 5 illustrate the course of stresses and table 2 presents numerical values of both stress and deformation.

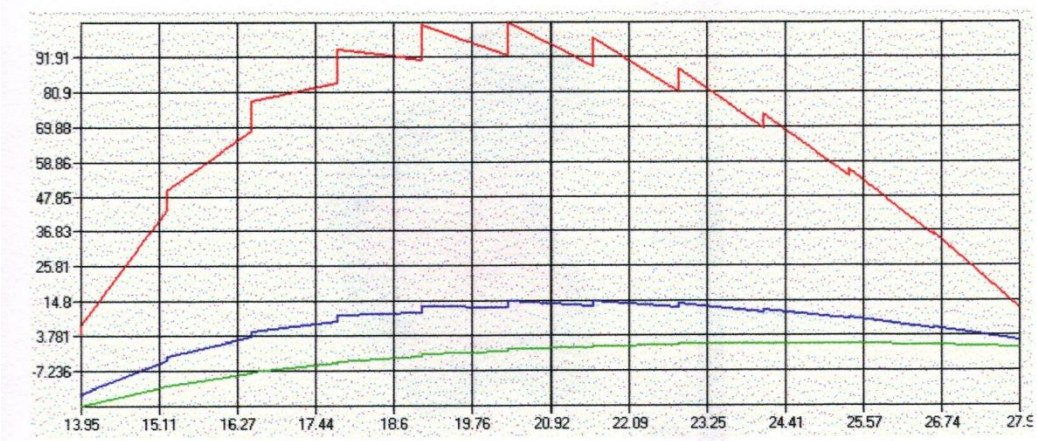

Figure 4 Hub. Radial stress [MPa] at 750 rpm (green), 3500 rpm (blue) and 6000 rpm (red)

The rotation induces a much more significant growth of stress in the hub. The equivalent stress von Mises for the hub gets close to the yield point around 3500 rpm (this is why the case of n = 6000 rpm was no longer taken into account).

The shape and value of stresses resulted through FEM analyses also confirm the theoretical approach.

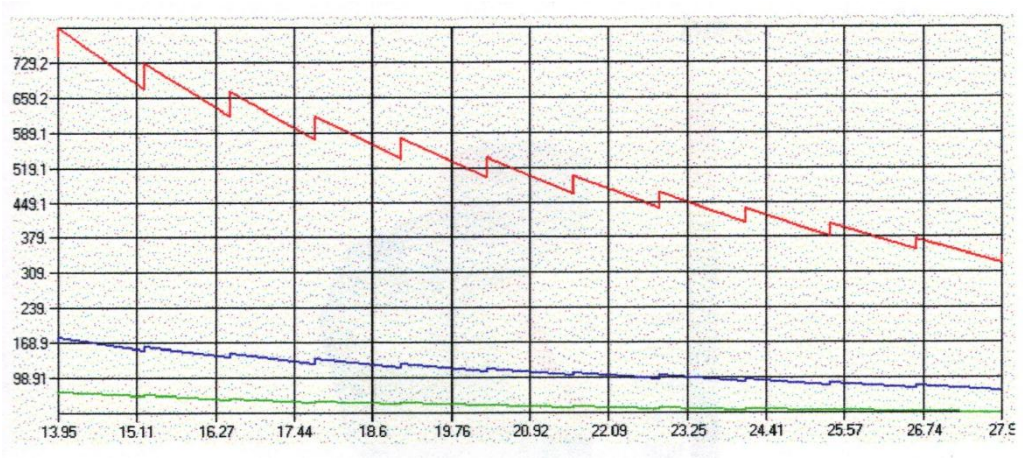

Figure 5 Hub. Tangential stress [MPa] at 750 rpm (green), 3500 rpm (blue) and 6000 rpm (red)

Table 2 Stress of hub, deformation of shaft and hub, effective interference, correction

n [rpm]	σ_r (r)/ σ_r (r_1) [MPa]	σ_t (r)/ σ_t (r_1) [MPa]	$\sigma_{von\ Mises}$ (r)/ $\sigma_{von\ Mises}$ (r_1) [MPa]	u_{hub} [μm]	u_{shaft} [μm]	s [μm] (effective MEF)	s_ω [μm] recommended [4]	s_ω [μm] effectively required
1	2	3	4	5	6	7	8	9
0	-19.54 -0.27	35.26 12.10	47.90 12.20	2.888	-1.320	4.208	0	0
750	-18.25 -0.20	71.90 27.82	87.75 27.62	8.830	-1.163	1.424	2.481	2.784
1500	-14.90 0.00	192.9 70.22	198.8 68.90	13.76	-0.750	-6.099	9.915	10.307
3500	4.10 16.00	854.8 314.2	843.2 306.9	59.43	+2.494	-48.522	54.031	52.730

Table 2 contains columns 5 – 9, which show the radial deformation of the hub at the contact surface (column 5), the radial deformation of the shaft at the contact surface (column 6), the effective value of the interference at a given angular velocity (column 7), the interference correction proposed in [4] - (column 8) and the interference correction effectively required according to MEF computation (column 9).

As the angular velocity increases, the effective interference results smaller and smaller. When both parts take positive deformations, the fit turns into a clearance fit.

Therefore, interference corrections are absolutely necessary.

Taking for reference value of interference the value corresponding to n = 0 rpm, s=4.208μm, it is possible to compute the required corrections depending on the angular velocity. The recommended values for the correction in [4] are written in column 8. One can notice a good similarity among the number in columns 8 and 9. Thus, corrections proposed in [4] can be used. However, a FEM analysis should provide more accurate values.

5. CONCLUSIONS

Stress and strain of the parts assembled through an interference fit can be computed based on analytical relationships, provided by the thick walled sleeves, in static regime.

Rotation movement, because of centrifugal forces changes the loading state. Deformations of shaft and hub take positive signs and the effective interference modifies. There is a critic value of the angular velocity, where the interference fit turns into a clearance one.

In order to preserve the required interference as resulted for static regime, it is compulsory to foresee a rotation correction. The analytical approaches of this problem are very few, because the actual shape of shaft, but especially hub are very different from thick walled sleeves. However, there are empirical recommendation for the case of shaft and hub manufactured from the same material.

A FEM analysis is the solution closest to real required interference.

The numerical application showed only a fair similarity between the values computed with the empirical recommended corrections and the values provided by the numerical simulation.

References:

1. Richard Budynas, Keith Nisbett, Shigley's Mechanical Engineering Design (Mcgraw-Hill Series in Mechanical Engineering) 8th ed., McGraw Hill Primis, USA, ISBN: 0−390−76487−6, 2006.
2. Manea, I. Organe de masini, vol. I: Editura Tehnica. Bucuresti. 1971.
3. Peeken, H. et al., MaschinenelementeVorlesungsumdruck, Band I: Trans-Aix-Press, Aachen, 1995.
4. Birger, I., et al., Rascet na procinosti, Detalii masini: Masinostroienie, Moscova, 1979.
5. Timosenko, S. P, et al., Theory of Elasticity, IIIrd Ed.: McGraw Hill Co, 1970.